World Journal of Engineering and Technology, 2024, 12, 587-616
https://www.scirp.org/journal/wjet
ISSN Online: 2331-4249
ISSN Print: 2331-4222

Nonlinear Time History Analysis for the Different Column Orientations under Seismic Wave Synthetic Approach

Mo Shi[1*], Peng Wang[2], Xiaoyan Xu[3], Yeol Choi[1]

[1]School of Architecture, Kyungpook National University, Daegu, Republic of Korea
[2]School of Computer Science and Technology, Shandong University, Qingdao, China
[3]HaXell Elevator Co., Ltd., Shanghai, China
Email: *shimo0204@outlook.jp

How to cite this paper: Shi, M., Wang, P., Xu, X.Y. and Choi, Y. (2024) Nonlinear Time History Analysis for the Different Column Orientations under Seismic Wave Synthetic Approach. *World Journal of Engineering and Technology*, **12**, 587-616.
https://doi.org/10.4236/wjet.2024.123038

Received: May 22, 2024
Accepted: July 26, 2024
Published: July 29, 2024

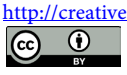

Abstract

The significant impact of earthquakes on human lives and the built environment underscores the extensive human and economic losses caused by structural collapses. Over the years, researchers have focused on improving seismic design to mitigate earthquake-induced damages and enhance structural performance. In this study, a specific reinforced concrete (RC) frame structure at Kyungpook National University, designed for educational purposes, is analyzed as a representative case. Utilizing SAP 2000, the research conducts a nonlinear time history analysis to assess the structural performance under seismic conditions. The primary objective is to evaluate the influence of different column section designs, while maintaining identical column section areas, on structural behavior. The study employs two distinct seismic waves from Abeno (ABN) and Takatori (TKT) for the analysis, comparing the structural performance under varying seismic conditions. Key aspects examined include displacement, base shear force, base moment, joint radians, and layer displacement angle. This research is anticipated to serve as a valuable reference for seismic restraint reinforcement work on RC buildings, enriching the methods used for evaluating structures through nonlinear time history analysis based on the synthetic seismic wave approach.

Keywords

Nonlinear Time History Analysis, Nonlinear Dynamic Analysis, Seismic Wave Synthetic, Seismic Restraint, RC Frame Structure, Column Orientation

1. Introduction

The perilous threat posed by earthquakes to civil infrastructure remains a press-

ing concern, underscored by a multitude of specific instances where seismic events have exacted a heavy toll on reinforced concrete (RC) structures worldwide [1]. A diverse array of researchers, drawing upon empirical evidence and historical precedents, highlight the critical danger posed by earthquakes to civil infrastructure [2].

The 1994 Northridge earthquake in the United States stands as a stark testament to the destructive power of seismic forces, causing widespread damage to RC buildings and infrastructure across Southern California. Similarly, the 1995 Kobe earthquake in Japan reverberated with catastrophic consequences [3]-[7]. After the millennium, the 2008 Wenchuan earthquake in China left an indelible scar on the landscape, claiming countless lives and inflicting extensive damage on RC frame structures throughout the region.

In recent studies, a lot of research emphasis has been placed on exploring the phenomenon of progressive collapse, which entails the sequential failure of structural elements following initial damage, leading to catastrophic structural failure. In this regard, Nonlinear Dynamic Analysis (NDA) has garnered considerable attention as a powerful tool for elucidating the complex interplay between seismic forces and structural vulnerabilities [8]. As a crucial aspect of nonlinear dynamic analysis (NDA), the nonlinear time history analysis stands out as a vital method for evaluating structural behavior during seismic events. This approach provides detailed insights into how structures respond to dynamic loads over time.

Unlike traditional linear analysis methods, as a significant aspect of nonlinear dynamic analysis (NDA), nonlinear time history offers a more nuanced perspective by accounting for nonlinear material behavior, geometric imperfections, and dynamic effects, thereby enabling a more accurate assessment of structural performance under earthquake loading [2] [8]. By simulating the time-varying response of structures subjected to seismic excitation, nonlinear time history analysis facilitates the identification of critical failure mechanisms, informing targeted interventions to enhance seismic resilience.

One of the key methodologies within NDA gaining prominence is nonlinear time history analysis, which involves subjecting structures to realistic earthquake ground motion records and evaluating their response over time [9]-[11]. This approach, characterized by its fidelity to real-world seismic events, provides invaluable insights into structural behavior under dynamic loading conditions.

Referring to the research of Phucuong Nguyen *et al.* [9], delves into the intricacies of structural damage induced by seismic events in El Centro, Northridge, and San Fernando. As depicted in **Figure 1**, the study harnesses the nonlinear time history analysis to comprehensively investigate the dynamic behavior and performance of buildings subjected to seismic forces.

Utilizing the structural analysis software SAP 2000, coupled with seismic wave data representative of the aforementioned earthquake events, the research endeavors to unravel the underlying mechanisms governing structural response to seismic loading. By simulating the time-varying dynamics of buildings under realistic seismic conditions, the study aims to elucidate critical insights into struc-

tural behavior, failure modes, and vulnerability thresholds.

Referring to the research by Mahapara Firdous *et al.* [10], this research employs nonlinear analytical methods to elucidate the influences on a specific educational RC frame structure in Kyungpook National University resulting from various column orientations. Furthermore, drawing upon the research contributions of Andi Yusra *et al.* [11] and Mahmood Hosseini *et al.* [1], the study extends its scope to encompass the multifaceted influences of different seismic waves, specifically Abeno (ABN) and Takatori (TKT), derived from the seismic events of the Kobe 1995 earthquake. Through the application of nonlinear time history analysis, this research seeks to compare and contrast the responses elicited by these seismic waves, thereby shedding light on the nuanced interactions between structural configurations, seismic excitation, and dynamic response. Throughout the results of this research, the findings of this research hold expect not only for bolstering the seismic resilience of RC buildings but also for advancing the frontiers of seismic analysis methodologies.

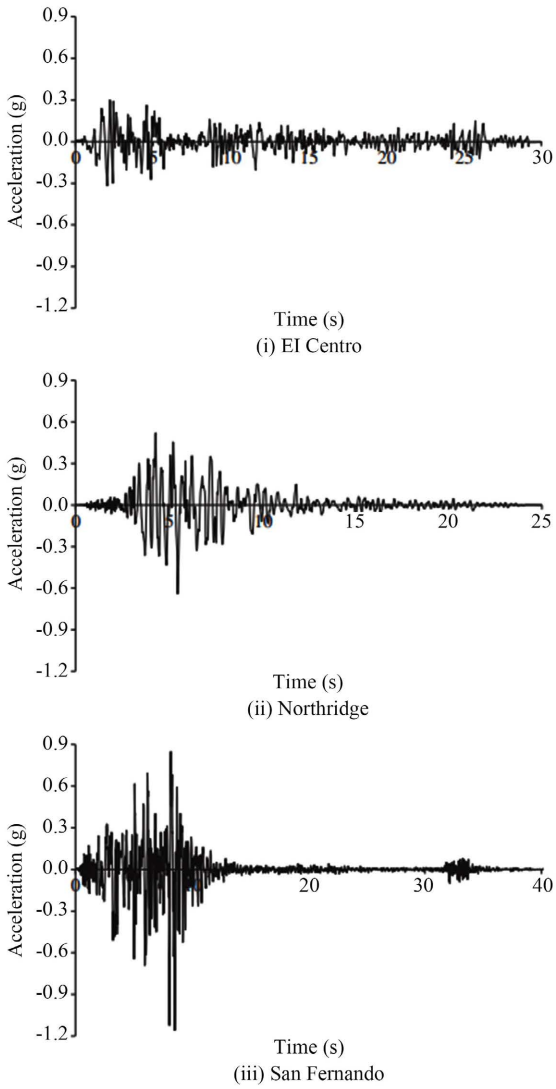

(a) Earthquake waves

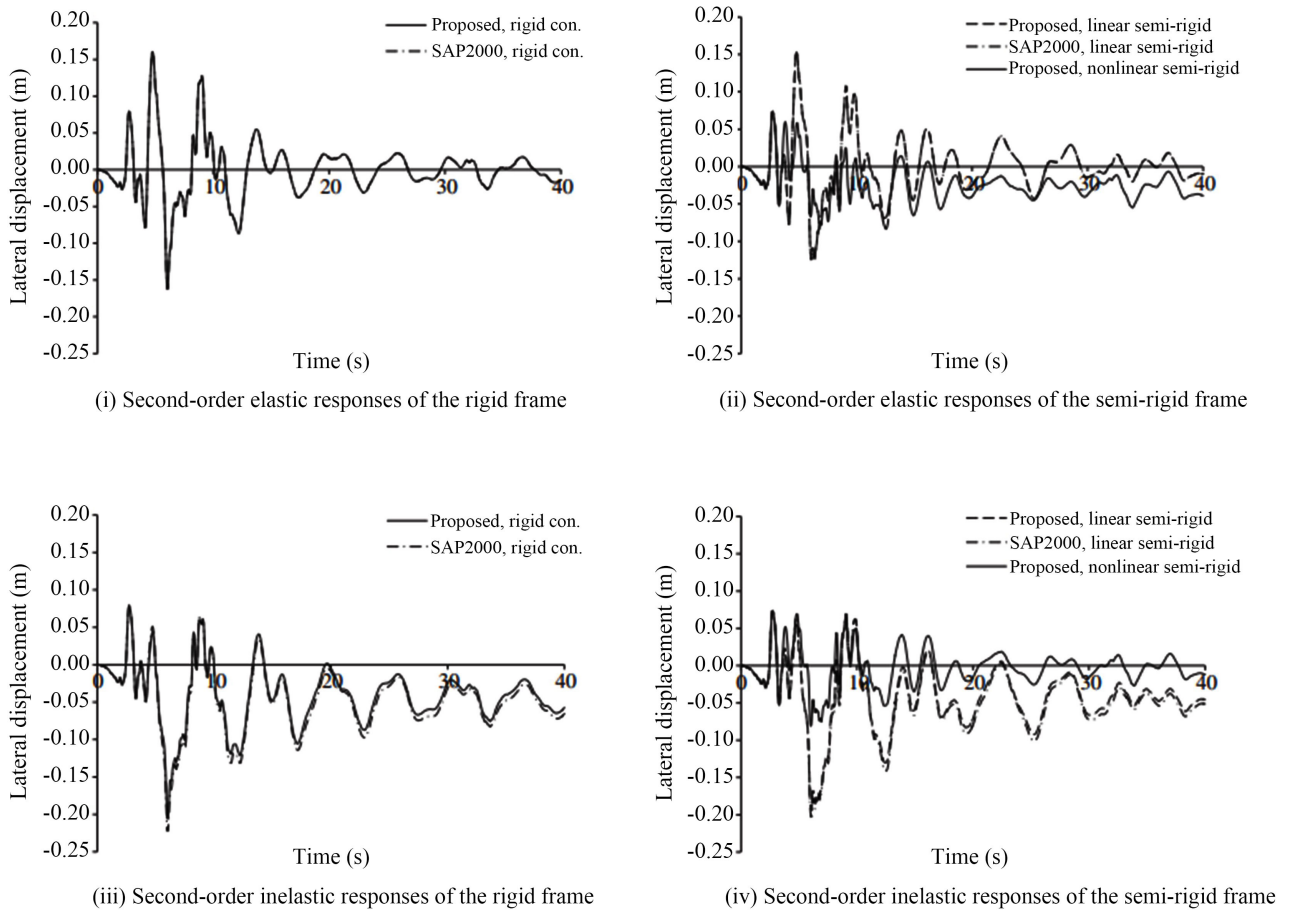

(i) Second-order elastic responses of the rigid frame

(ii) Second-order elastic responses of the semi-rigid frame

(iii) Second-order inelastic responses of the rigid frame

(iv) Second-order inelastic responses of the semi-rigid frame

(b) Nonlinear time history responses

Figure 1. Nonlinear time-history analysis based on seismic waves.

2. Description of the Research

2.1. Structure Description

This research endeavors to conduct a comprehensive analysis of an educational building dating back to the 1970s, focusing specifically on an RC frame structure nestled within the Department of Architectural Engineering at Kyungpook National University, strategically situated within Daegu Metropolitan City, Republic of Korea. The selected building's geographical coordinates are situated at a longitude of 128˚60'85"E and a latitude of 35˚88'76"N. The coordinates serve as the geographical reference points essential for contextualizing the research findings within the unique seismic and environmental conditions prevalent in the region.

Numerous previous research, such as Riza Ainul Hakim *et al.* [12] and S. C. Pednekar *et al.* [13], have highlighted the crucial role of structural regularity in RC frame structures for effective structural analysis. Consequently, to compare with other irregular RC structures, the regularity of the RC frame structure of the Department of Architectural Engineering at Kyungpook National University is expected to reduce variables due to the RC frame structure itself, and also ex-

pected to analyze the influences of the column section orientation for the specific RC frame structure under the specific seismic wave.

The RC frame structure for this research, as illustrated in Figure 2, constitutes an architectural entity occupying a total area of 1316 m^2. The structure spans a length of 70 m, encompassing a breadth of 18.8 m and soaring to a height of 18.3 m. Classrooms flanking the periphery of the structure are crafted with those on the sides measuring 7 m in length and 4.5 m in width, while larger classrooms boast dimensions of 9 m by 4.5 m. Upon inspection of the 3D model in SAP 2000 as Figure 2(b) illustrates, it becomes evident that the RC frame configuration encompasses four stories, each maintaining a uniform height of 3.5 m. Furthermore, a final stair room is situated atop the roof, ascending to a height of 3.8 m.

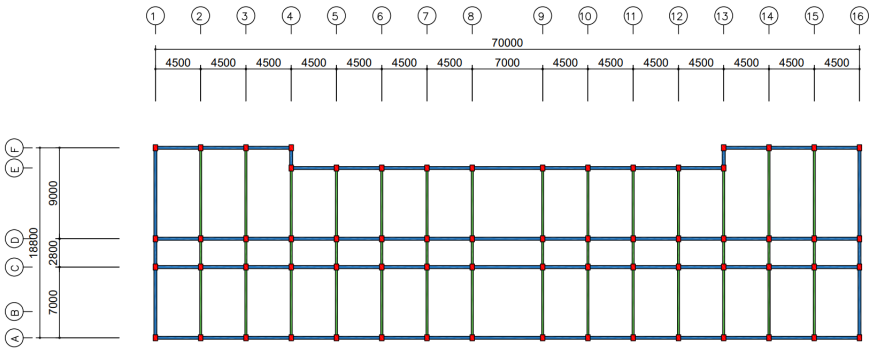

(a) Floor Plan

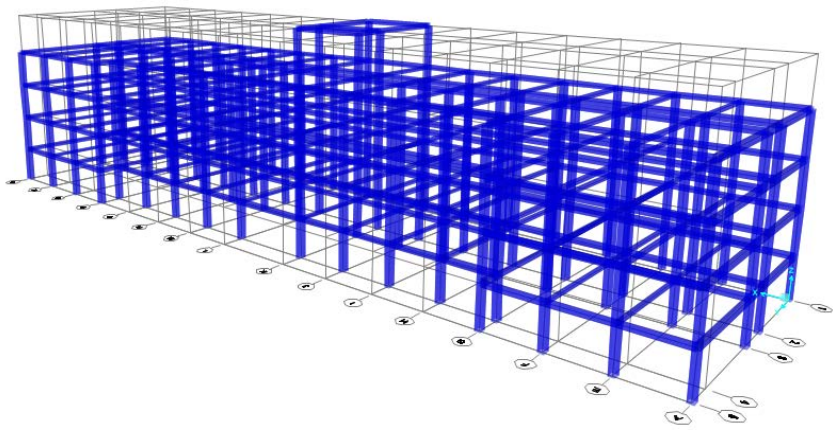

(b) 3D model in SAP 2000

Figure 2. Design of the specific RC frame structure.

Figure 3 offers a comparative depiction of the design nuances inherent in columns sharing a common cross-sectional area of 270,000 m^2. The columns in this research are categorized into two distinct cases: CASE-1, characterized by dimensions of 450 mm × 600 mm, and CASE-2, featuring dimensions of 600 mm × 450 mm. While both cases maintain the same cross-sectional area, the differing orientations offer a unique opportunity to explore how variations in column orientations influence structural behavior and performance.

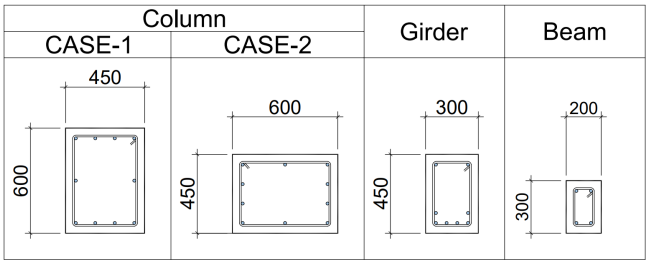

Figure 3. The section designs (Unit: mm).

Within each column section, an arrangement of reinforcing rebars is employed to enhance structural robustness and resilience. Specifically, ten longitudinal D19 rebars are positioned within the column section, complemented by D10 hoop rebars spaced at 300 mm intervals. Moreover, referring to the standards outlined in KDS 14 20 50: 2022, a regulatory framework, dictates a concrete covering depth of 40 mm for the reinforcing bars.

The girder is an integral component of the RC frame structure under examination, with a cross-sectional area of 135,000 mm^2, measuring 300 mm in width and 450 mm in height. To fortify the girder against bending and shear forces, the design of the girder section comprises a total of eight longitudinal rebars. At the top, two robust D16 rebars are strategically positioned to withstand tensile forces and bending moments, providing essential reinforcement against vertical loads and structural deflections. Similarly, at the bottom of the girder, six D16 rebars are deployed to enhance compressive strength and structural rigidity, effectively counteracting the gravitational forces exerted on the structure. In addition to longitudinal reinforcement, the girder incorporates hoop rebars D10 spaced at 300 mm intervals, placed to enhance structural stability and ductility. Adhering to industry standards, the concrete cover depth of the girder strictly complies with the guidelines outlined in KDS 14 20 50: 2022 as maintaining a concrete cover depth of 40 mm.

The beam is also a vital structural element within the RC frame system with a cross-sectional area meticulously crafted to 60,000 mm^2. The section of the beam measures 200 mm in width and 300 mm in height. To fortify the beam against bending and shear forces comprising four longitudinal rebars. At the top, two D16 rebars are positioned to withstand tensile forces and bending moments, providing essential reinforcement against vertical loads and structural deflections. Similarly, at the bottom of the beam, two D16 rebars are deployed to enhance compressive strength and structural rigidity, effectively counteracting the gravitational forces exerted on the structure. In addition to longitudinal reinforcement, the beam incorporates hoop rebars D10 placed at 300 mm intervals, serving to enhance structural stability and ductility. Adhering to established industry standards, the concrete cover depth of the beam aligns with the guidelines outlined in KDS 14 20 50: 2022, maintaining a depth of 40 mm.

Adhering to the rigorous requirements outlined in KS F 4009:2021 for ready-mixed concrete as Table 1 illustrates, the concrete used in this research meets industry standards for consistency, durability, and performance.

Table 1. Design of column, girder, and beam.

Concrete	Weight per unit volume		23540 N/m^3	
	Mass per unit volume		2400 kg/m^3	
	Modulus of elasticity		22334 MPa	
	Poisson		0.1667	
	Coefficient of Thermal expansion		1.100E−05	
	Specified Compressive Strength		15.12 MPa	
	Expected Compressive Strength		18.14 MPa	
Rebar	Weight per unit volume		77000 N/m^3	
	Mass per unit volume		7850 kg/m^3	
	Modulus of elasticity		200000 MPa	
	Poisson		0.3	
	Coefficient of Thermal expansion		1.170E−05	
	Minimum Stress		240 MPa	
	Expected Stress		300 MPa	
Column	Longitudinal Rebar	8-D19 & 2-D16	Stiffness of Shear	0.45
	Hoop Rebar	D10@300	Stiffness of Moment	0.70
Girder	Longitudinal Rebar	8-D16	Stiffness of Shear	0.45
	Hoop Rebar	D10@300	Stiffness of Moment	0.35
Beam	Longitudinal Rebar	4-D16	Stiffness of Shear	0.45
	Hoop Rebar	D10@300	Stiffness of Moment	0.35

Description of rebar size: D indicates rebar diameter
D19, D16, and D10 refer to rebar diameters of 19 mm, 16 mm, and 10 mm, respectively

Aligned with the design guidelines prescribed by the Ministry of Education of the Republic of Korea for educational buildings dating back to the 1980s, the specified compressive strength of the concrete is denoted as F_{ck} = 15.12 MPa. The expected compressive strength of the concrete, represented by F_{ek} = 18.14 MPa, offers a glimpse into its potential performance under real-world conditions, accounting for factors such as curing time, environmental influences, and quality control measures.

Drawing from the guidelines outlined in KS D 3504:2021 for steel bars utilized in concrete reinforcement, and informed by the educational building design specifications of the 1980s by the Ministry of Education of the Republic of Korea, the strength of the rebar is designated as F_y = 240 MPa. In addition to the designated strength value, the anticipation of stress, denoted as F_{ey} = 300 MPa, provides a valuable parameter for evaluating the steel bar's expected performance under various load conditions.

In adhering to design principles reminiscent of typical school buildings from the 1980s and drawing guidance from Table 5.3.1 in KISTEC 2021, specific shear and moment stiffness values are meticulously specified for both column and beam sections. Referring to Table 1, a shear stiffness of 0.45 and a moment stiffness of 0.7 are designated for the column section, emphasizing the structure's capacity to resist bending and axial loads. Conversely, the girder and beam section design features a shear stiffness of 0.45 and a relatively lower moment

stiffness of 0.35, reflecting a configuration that is more responsive to shearing forces and lateral loads.

Assigning plastic hinge properties to structural components in SAP 2000 is essential, following ASCE 41-13 guidelines. Column decisions are based on Table 10-8 for Reinforced Concrete Columns in nonlinear procedures, focusing on Condition ii-Flexure/Shear with axial forces and bending moments about the M2 and M3 axes. Plastic hinge modeling for girders and beams follows ASCE 41-13 guidelines, specifically Table 10-7 for Reinforced Concrete Beams, focusing on the M3 degree of freedom to understand the response to lateral forces.

2.2. Load Design

Following industry standards outlined in Table 0303.2.1 of KBC 2016, the Dead Load and Live Load specifications for the educational usage structure of the school building are meticulously delineated.

The Dead Load represents the weight of the building's permanent components and materials and is specified as 4.3 kN/m^2. In contrast, the Live Load, which accounts for the transient or variable loads imposed by occupants, furniture, equipment, and temporary installations, is allocated a value of 3 kN/m^2. Furthermore, the Live Load specifically on the corridor is designed to be slightly higher at 4.0 kN/m^2, reflecting the anticipated higher foot traffic and dynamic loads experienced in this area.

In addition to Dead Load and Live Load considerations, roof load calculations must also account for environmental factors such as snow accumulation. As depicted in Figure 4 and elaborated in KBC 2016, a snow load of 0.5 kN/m^2 is factored into roof load considerations.

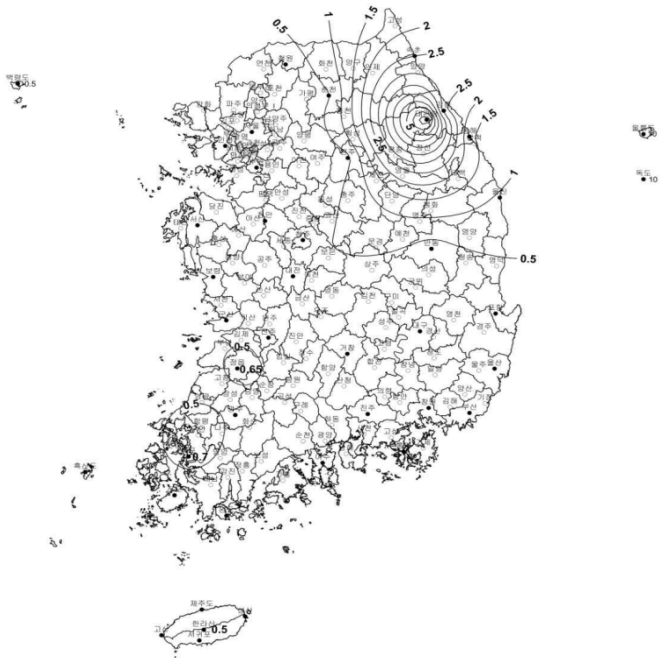

Figure 4. Design of the snow load (KBC 2016).

Subsequently, by taking into account the dimensions of each room of the specific RC frame structure, the calculations for the Dead Load, Live Load, and Snow Load can be performed using the formulas provided below:

$$\omega_D = P_D / L \tag{1}$$

$$\omega_L = P_L / L \tag{2}$$

where P_D represents the Dead Load force, and ω_D signifies the uniform load from the Dead Load. Conversely, P_L denotes the Live Load force, and ω_L represents the uniform load from the Live Load. Utilizing these calculations, the Dead Load, Live Load, and Snow Load can be calculated as Table 2 shows.

Table 2. Structure of the train network.

Room	Length	KBC 2016			Dead Load		Live Load		Snow Load (Roof)	
		Dead Load	Live Load	Snow Load	P_D	ω_D	P_L	ω_L	P_L	ω_L
	m	kN/m²	kN/m²	kN/m²	kN/m	kN/m	kN/m	kN/m	kN/m	kN/m
Small	4.5	4.3	3	0.5	21.77	4.838	15.19	3.38	2.53	0.56
	7	4.3	3	0.5	52.68	7.525	36.75	5.25	6.13	0.88
Middle	4.5	4.3	3	0.5	21.77	4.838	15.19	3.38	2.53	0.56
	9	4.3	3	0.5	87.08	9.675	60.75	6.75	10.13	1.13
Large	7	4.3	3	0.5	52.68	7.525	36.75	5.25	6.13	0.88
	7	4.3	3	0.5	52.68	7.525	36.75	5.25	6.13	0.88
Corridor	2.8	-	4	0.5	-	-	7.84	2.8	0.98	0.35
	7	-	4	0.5	-	-	49.00	7	6.13	0.88
	4.5	-	4	0.5	-	-	20.25	4.5	2.53	0.56

2.3. Nonlinear Time History Analysis

Based on the findings of many former researchers regarding the Kobe 1995 earthquake [3]-[5], this research draws upon the seismic wave data obtained from two observation stations: Abeno (ABN) and Takatori (TKT) on January 16, 1995.

The seismic wave data from Abeno (ABN) is particularly extensive, comprising a dataset consisting of 14,000 recorded points, meticulously sampled at regular intervals of 0.01 seconds. As a comparison, the seismic wave data from Takatori (TKT) provides valuable recorded data, consisting of 4,096 recorded points sampled at identical intervals of 0.01 seconds. Figure 5 serves as an essential visual aid, presenting the Acceleration and Time results derived from the analysis of these specific seismic wave datasets.

Figure 5 provides a visual representation of the recorded seismic waves in Abeno (ABN) and Takatori (TKT), offering critical insights into the seismic characteristics observed at these distinct locations during the Kobe 1995 earthquake. One striking difference revealed by Figure 5 is the wave recorded in

Abeno spans a total of 140 seconds, significantly longer than the 40 seconds recorded in Takatori. Moreover, Figure 5 highlights notable disparities in the magnitudes of acceleration between Abeno and Takatori. In Takatori, the seismic wave exhibits substantially larger accelerations, with maximum positive and negative accelerations reaching 0.61771 g and −0.54284 g, respectively, at specific time intervals. In comparison, the accelerations recorded in Abeno are comparatively smaller, with maximum positive and negative accelerations of 0.14866 g and −0.22063 g, respectively. These variations in acceleration magnitudes underscore the diverse seismic intensities experienced at different locations within the earthquake-affected region.

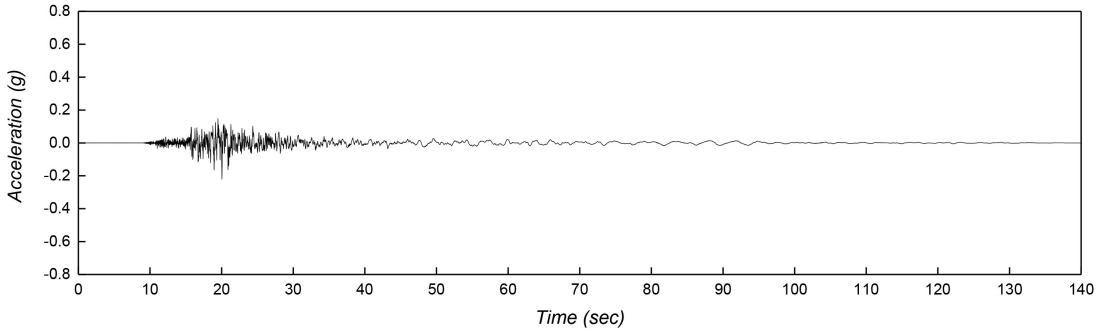

(a) Seismic wave in Abeno (ABN)

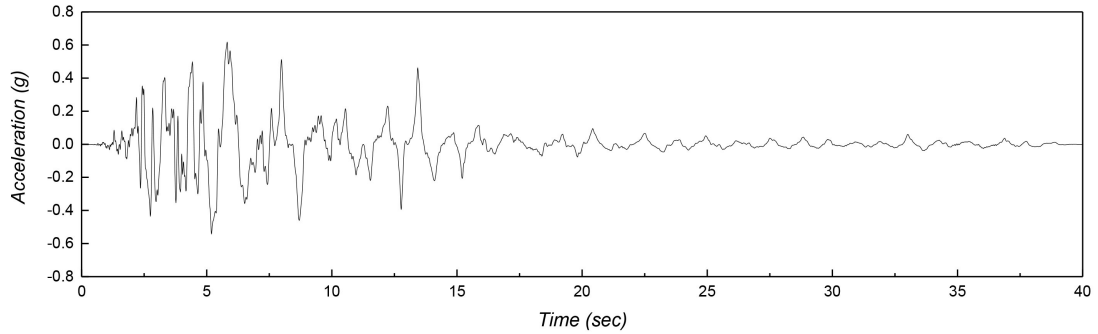

(b) Seismic wave in Takatori (TKT)

Figure 5. Seismic waves of Kobe 1995 earthquake.

Given these significant differences in both duration and acceleration between the seismic waves recorded in Abeno and Takatori, it becomes imperative to examine their implications for structural behavior. The utilization of nonlinear time history analysis offers a meaningful approach for elucidating these differences and understanding their impact on the response of structures subjected to the Kobe 1995 earthquake.

Figure 6 provides a detailed analysis of the velocity characteristics associated with the seismic waves recorded in Takatori and Abeno during the Kobe 1995 earthquake, shedding light on the dynamic behavior of these waves and their implications for structural response. One finding highlighted by Figure 6 is the stark contrast in velocity between the two seismic waves, with the wave observed

in Takatori exhibiting notably faster velocities compared to Abeno.

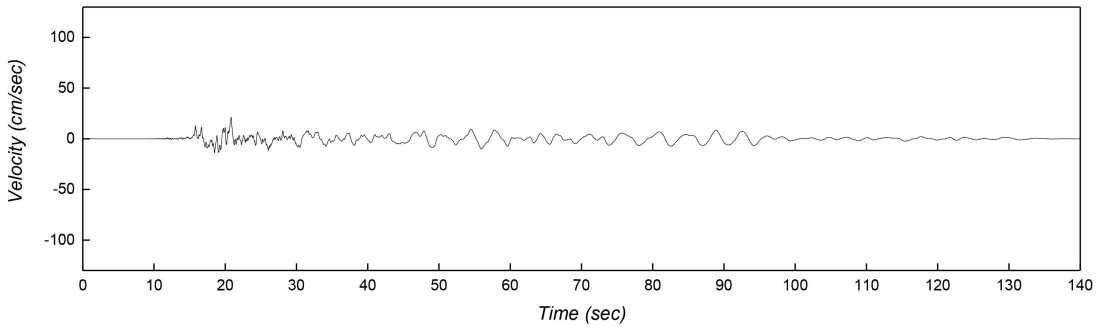

(a) Seismic wave in Abeno (ABN)

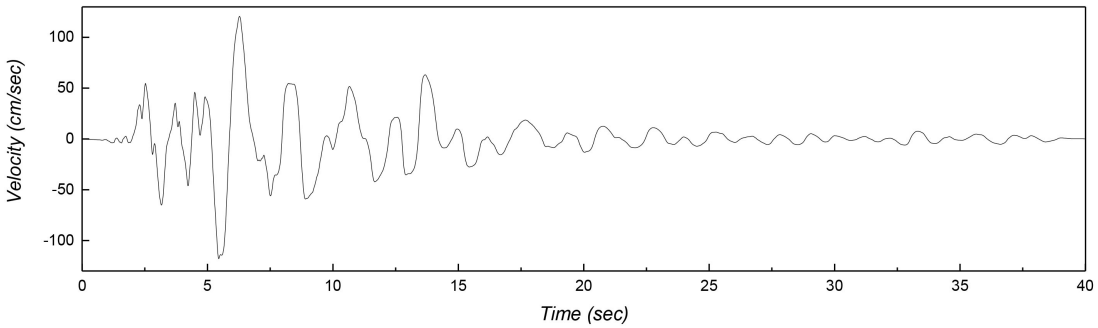

(b) Seismic wave in Takatori (TKT)

Figure 6. Velocity of seismic waves.

In Takatori, the analysis reveals that the seismic wave attains maximum velocities of 120.68 cm/sec and −117.91 cm/sec for the positive and negative zones, respectively. In contrast, the velocities recorded in Abeno are notably lower, with maximum velocities reaching 21.49 cm/sec and −13.95 cm/sec for the positive and negative zones, respectively.

The analytical exploration of seismic characteristics extends beyond velocity to include displacement, offering further insights into the dynamic response of structures to seismic waves. As **Figure 7** illustrates, the analysis reveals a clear pattern: Takatori experiences significantly larger displacements compared to Abeno, attributable to the faster acceleration and velocity observed in Takatori.

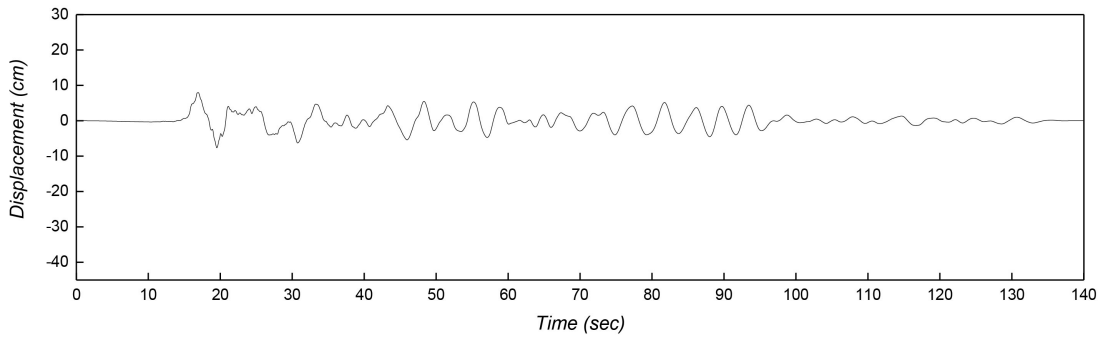

(a) Seismic wave in Abeno (ABN)

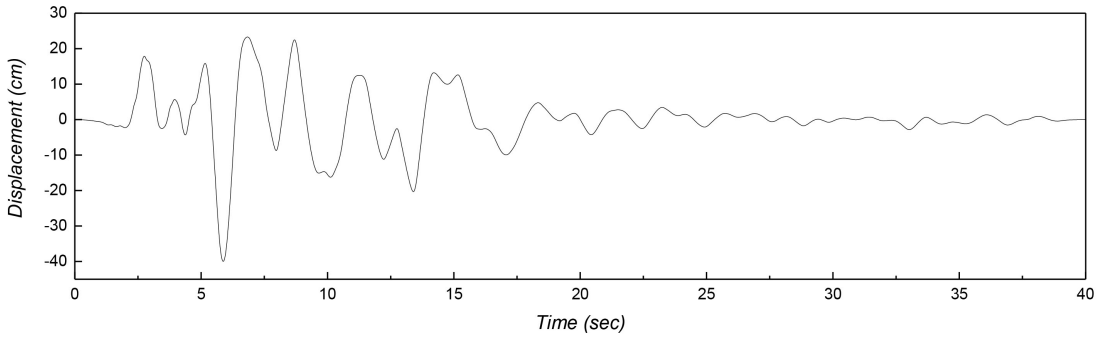

(b) Seismic wave in Takatori (TKT)

Figure 7. Displacement of seismic waves.

In Takatori, the seismic displacement reaches maximum values of 23.30 cm and −39.95 cm for the positive and negative zones, respectively. In contrast, the displacements recorded in Abeno are notably smaller, with maximum values reaching 7.98 cm and −7.62 cm for the positive and negative zones, respectively.

In the quest to accurately simulate the seismic behavior observed during the Kobe 1995 earthquake, this research harnesses nonlinear time history analysis, capable of generating synthetic time histories that closely resemble the actual seismic events recorded at specific observation points. The process begins by leveraging the reference acceleration data obtained from two critical observation points: Abeno (ABN) and Takatori (TKT).

Furthermore, This synthetic time history is created in both the frequency domain and time domain, aligning with the target response spectrum specified in KBC 2016, as the site class of SD, where site coefficient F_a (Acceleration responses of the soil to short periods) is 1.46, and F_v (acceleration responses of the soil to long periods) is 1.58. Then, the value of S_{DS} (Short-Period Spectral Response Acceleration) and S_{D1} (1-second Spectral Response Acceleration) can be calculated as the equation shown below:

$$S_{D1} = S \times F_v \times 2/3 \tag{3}$$

$$S_{DS} = S \times 2.5 \times F_a \times 2/3 \tag{4}$$

where S represents the effective ground acceleration value for a 2400-year return period earthquake, sourced from Table 0306.3.1 of KBC 2016, and the value of F_a and F_v gives 1.46 and 1.58 respectively. Applying the provided equations, the 1-sec spectral acceleration is computed as 0.22 g, while the 0.2-sec spectral acceleration stands at 0.55 g.

The synthetic seismic wave approach in nonlinear time history analysis involves generating artificial earthquake records that are used as input ground motions for the dynamic analysis of structures. This method is crucial for assessing the performance and safety of structures under seismic loads, especially when real earthquake records are scarce, not representative of the site conditions, or when specific design earthquake scenarios need to be considered [14] [15].

Synthetic seismic waves can be generated to match specific design spectra or site conditions, providing more relevant and controlled input for analysis. Also,

this approach enables the study of hypothetical earthquake scenarios, including rare or extreme events that may not be represented in historical records [14]. Furthermore, this approach offers consistency and reproducibility, which is beneficial for comparative studies and design validation.

Achieving an accurate representation of seismic events requires the synthesis of matching time history data that captures seismic characteristics across both frequency and time domains. This synthesis process, exemplified in **Figure 8**, plays a pivotal role in ensuring the analytical results and enhancing the understanding of structural response to seismic loading.

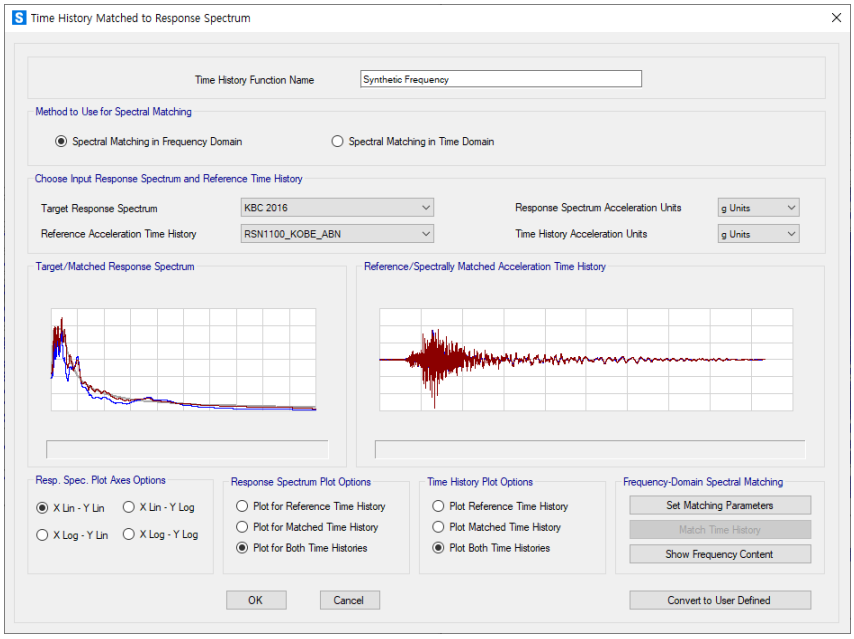

(a) Synthetic Frequency—ABN

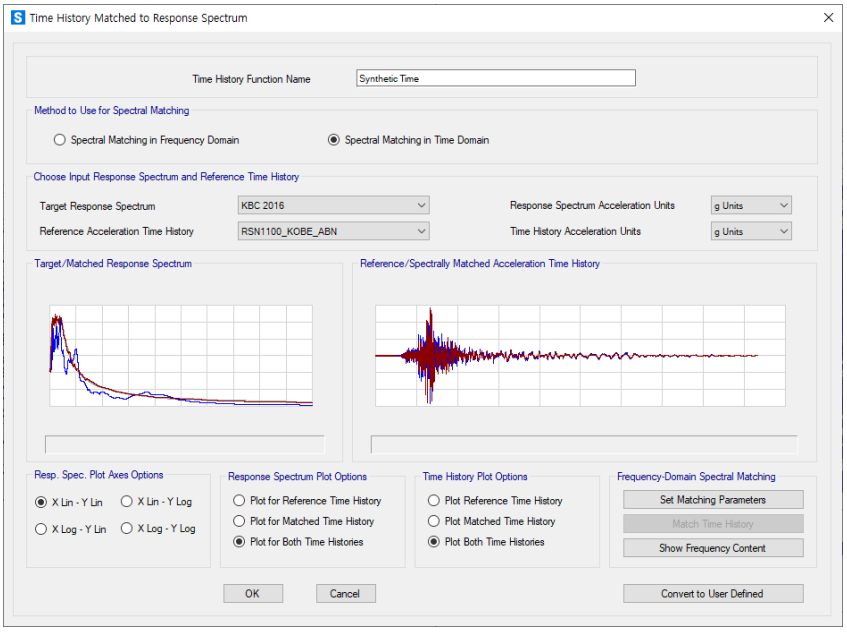

(b) Synthetic Time—ABN

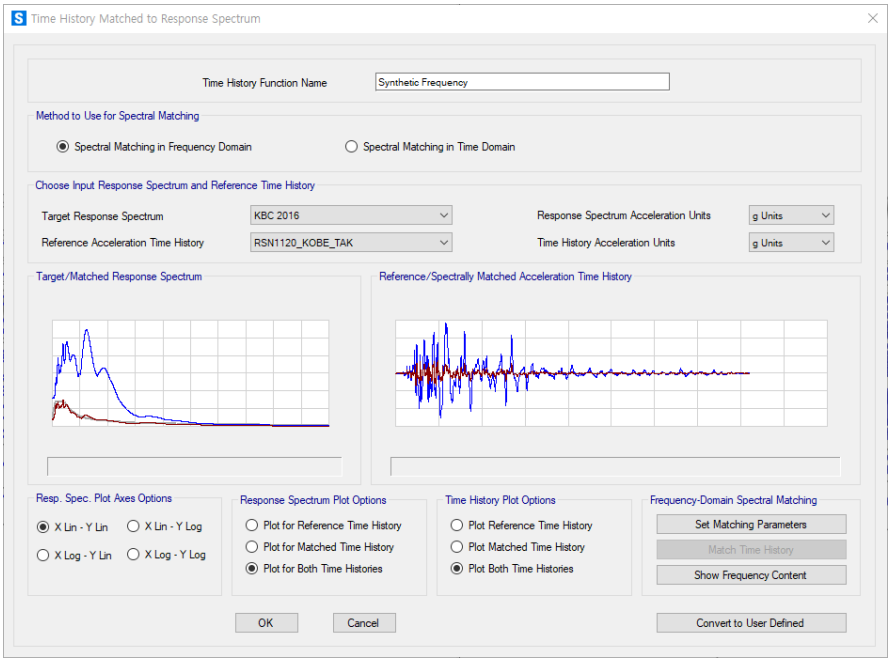

(c) Synthetic Frequency—TKT

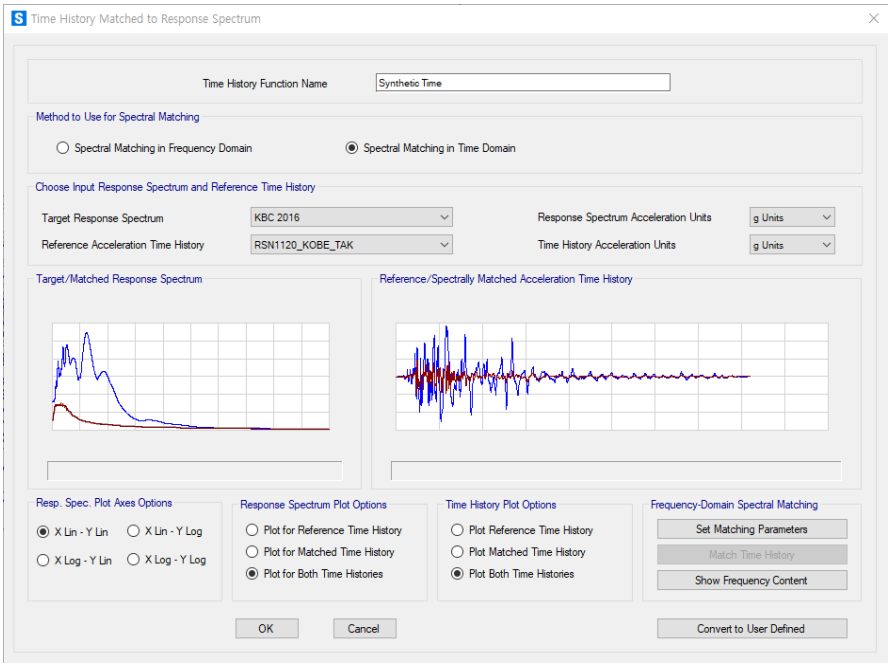

(d) Synthetic Time—TKT

Figure 8. Approach of nonlinear time history analysis.

Referring to **Figure 8**, despite variations in the magnitude of seismic waves between Takatori (TKT) and Abeno (ABN), the synthetic results exhibit remarkable similarities. This result can be attributed to the utilization of the same target response spectrum specified in KBC 2016. Due to this, this research is expected to gain similar results under the nonlinear time history analysis for the specific RC frame structure.

3. Discussion of the Analysis

3.1. Base Shear, Base Moment, and Displacement

The research emphasizes the importance of nonlinear time history analysis in seismic performance studies, particularly focusing on the Kobe 1995 earthquake. Nonlinear time history analysis is applied using seismic waves from Abeno (ABN) and Takatori (TKT). The synthetic response spectrum is generated through a response spectrum synthetic approach in SAP 2000, based on the Kobe 1995 earthquake seismic waves of Abeno (ABN) and Takatori (TKT) respectively, aligning with the specific response spectrum of KBC 2016. The analysis introduces positive and negative zones, resulting in eight analytical datasets derived using spectral matching methods in both frequency and time domains, illustrated in Figure 9.

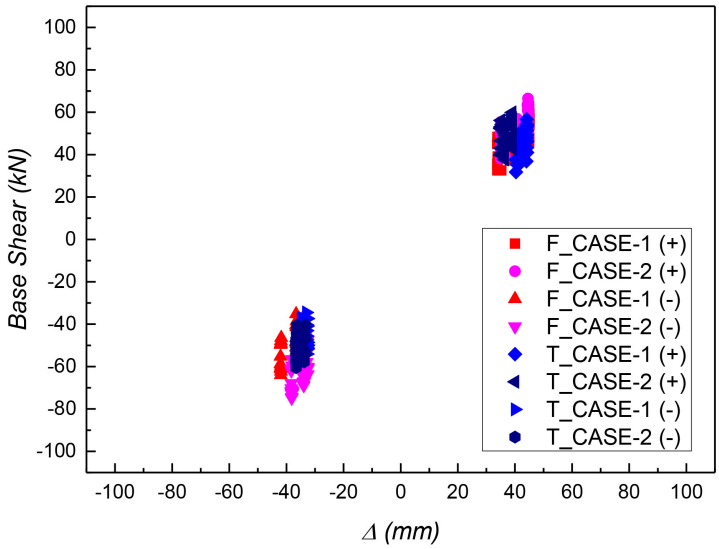

(a) ABN-Direction x

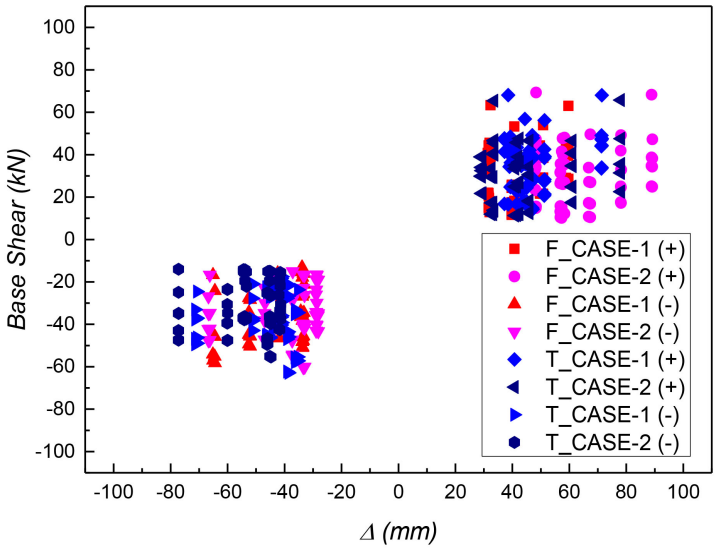

(b) ABN-Direction y

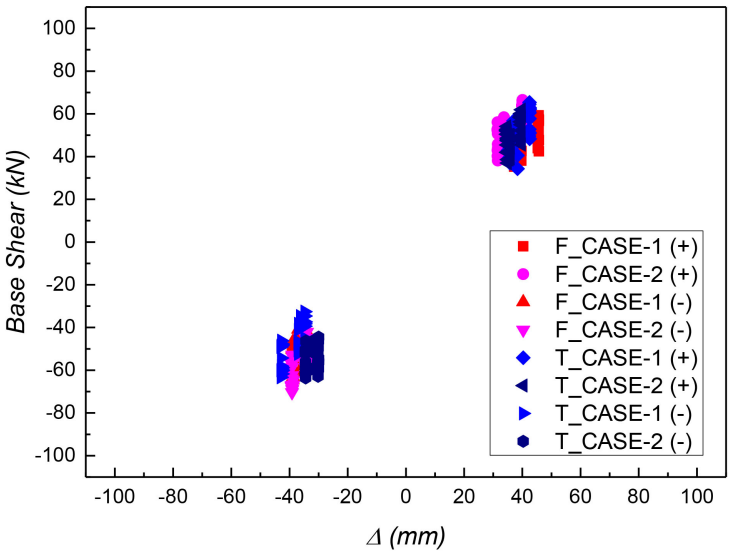

(c) TKT-Direction x

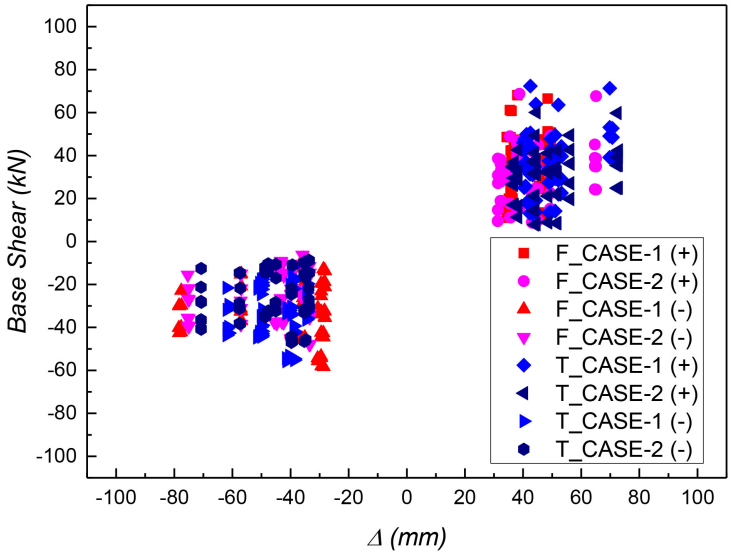

(d) TKT-Direction y

Figure 9. Base shear and displacement.

In the realm of seismic analysis, understanding the structural response of buildings is paramount for ensuring their safety and resilience. Involving a total of 66 points positioned across both the foundation and roof of the RC frame structure under study, this research emphasizes evaluating structural performance by examining two critical parameters: base shear force and roof displacement. The collection of base shear force values from all foundation points allows for a comprehensive analysis of seismic forces acting on the structure. Under the two different seismic waves of Abeno (ABN) and Takatori (TKT), the division of results into x and y directions provides a detailed understanding of how seismic forces vary spatially. Simultaneously, the monitoring of displacement at 66 points on the roof offers insights into the dynamic behavior of the

structure during seismic events. Figure 9 serves as a visual representation of the interplay between the base shear force on the foundation and displacement on the roof.

Figure 9 presents a comparative analysis of base shear and displacement for different column orientations, particularly focusing on CASE-1 and CASE-2. In the x-direction, CASE-2 shows higher base shear, while CASE-1 exhibits slightly longer displacement. Conversely, in the y-direction, CASE-1 surpasses CASE-2 in base shear, while CASE-1 exhibits slightly shorter displacement. This underscores the sensitivity of structural response to column section designs. These consistent findings across spectral matching approaches in both frequency and time domains, validated by Abeno (ABN) and Takatori (TKT) seismic waves, affirm the results. Figure 9 visually illustrates the findings for both different directions and both different seismic waves.

In the analysis of base moment, graph (a) and graph (c) within Figure 10 demonstrate that CASE-1 exhibits a larger base moment when the analysis is conducted in the x direction. This suggests that the orientation of CASE-1's column sections provides greater resistance to seismic forces in this specific direction. Conversely, graph (b) and graph (d) show that CASE-2 demonstrates a larger base moment when analyzed in the y direction. This indicates that CASE-2's column orientation is more effective in resisting seismic forces from this angle. The divergence of the results highlights the sensitivity of the structural response to the orientation of the analysis, underscoring the importance of considering directional influences in column design. By employing two distinct approaches—Frequency Domain and Time Domain—the research confirms that the analysis of base moment and displacement yields identical results under the seismic waves of the Kobe 1995 earthquake in both Abeno and Takatori, and this consistency reinforces the reliability of the synthetic methods used and provides a robust basis.

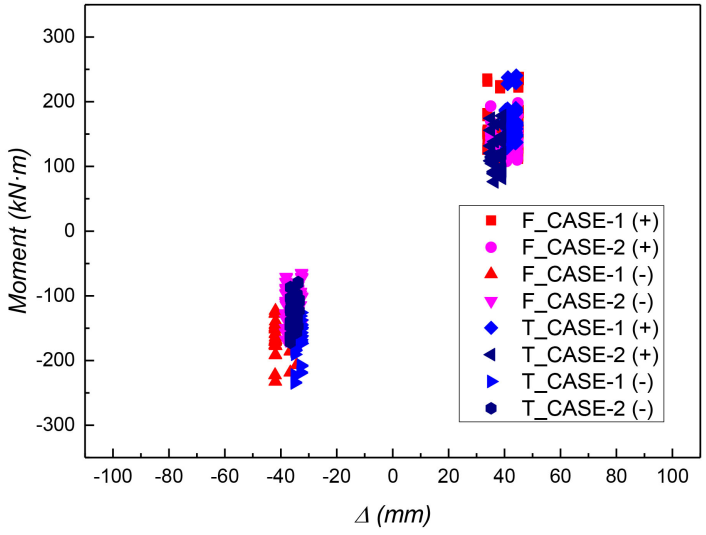

(a) ABN-Direction x

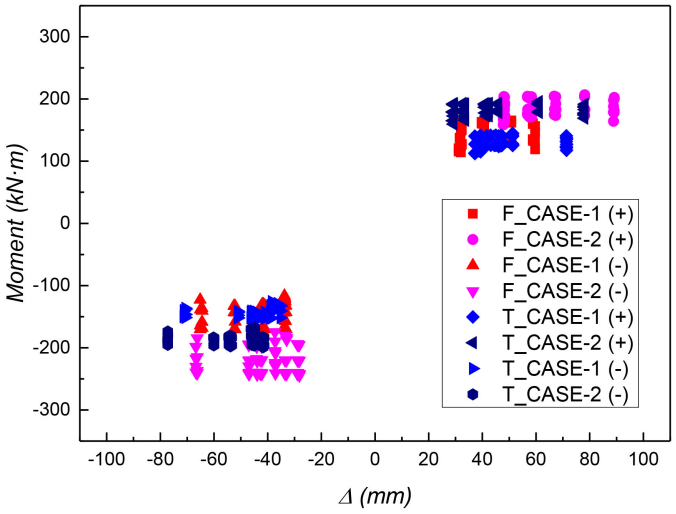

(b) ABN-Direction y

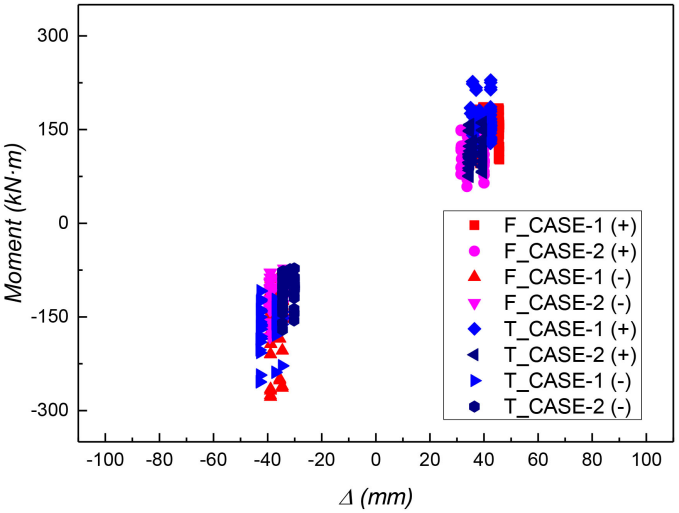

(c) TKT-Direction x

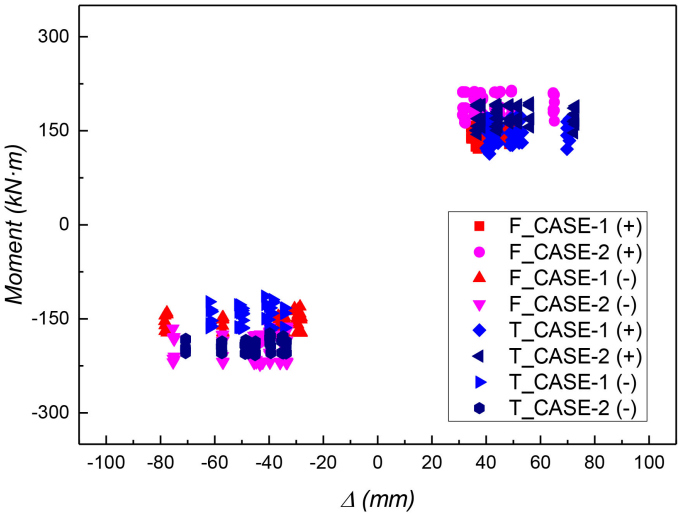

(d) TKT-Direction y

Figure 10. Base moment and displacement.

3.2. Layer Displacement and Radians

The findings depicted in Figure 11 and Figure 12 emphasize the critical role of displacement and radians analysis in assessing structural performance during seismic events. Figure 11 visually demonstrates that, based on the seismic waves from Abeno and Takatori, CASE-1 exhibits a longer average displacement in the x-direction. This indicates that the column design in CASE-1 is more susceptible to movement along the x-direction. Conversely, in the y-direction, CASE-2 shows a longer average displacement, suggesting that its column configuration is more prone to displacement in the y-direction.

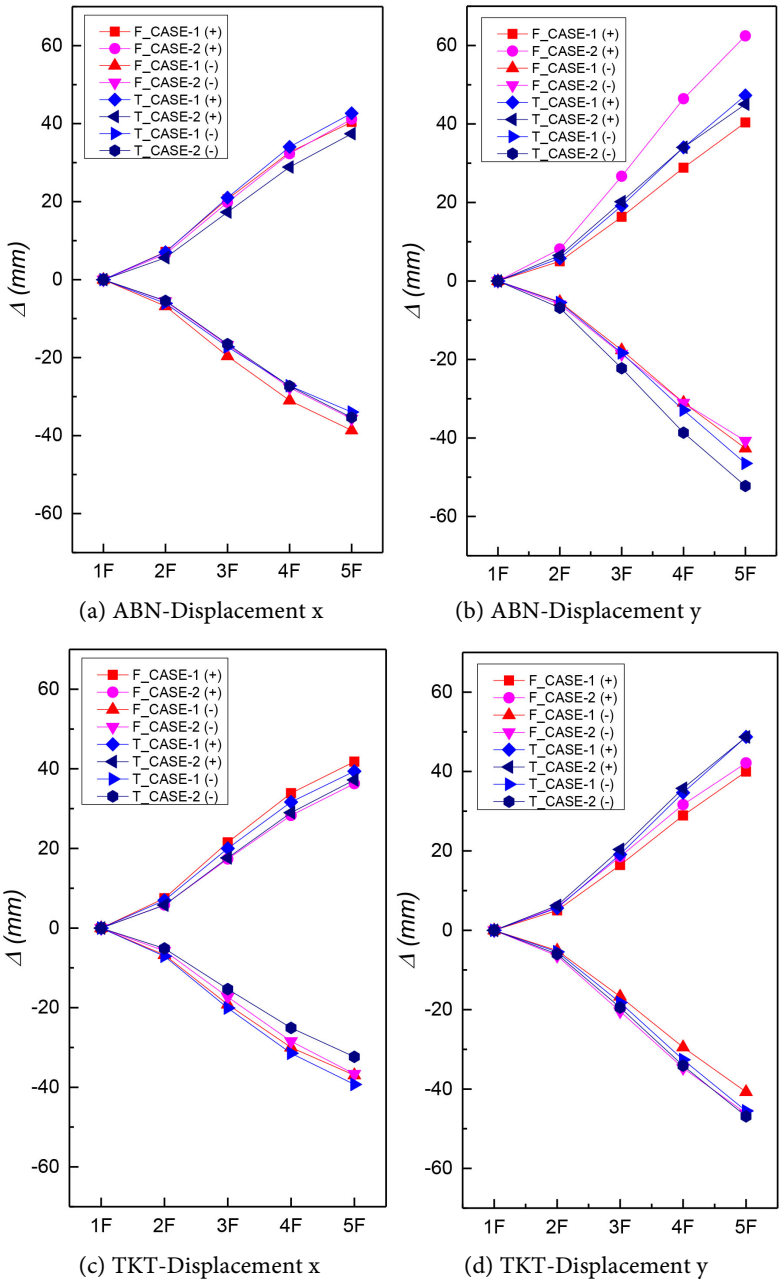

(a) ABN-Displacement x

(b) ABN-Displacement y

(c) TKT-Displacement x

(d) TKT-Displacement y

Figure 11. Average displacement.

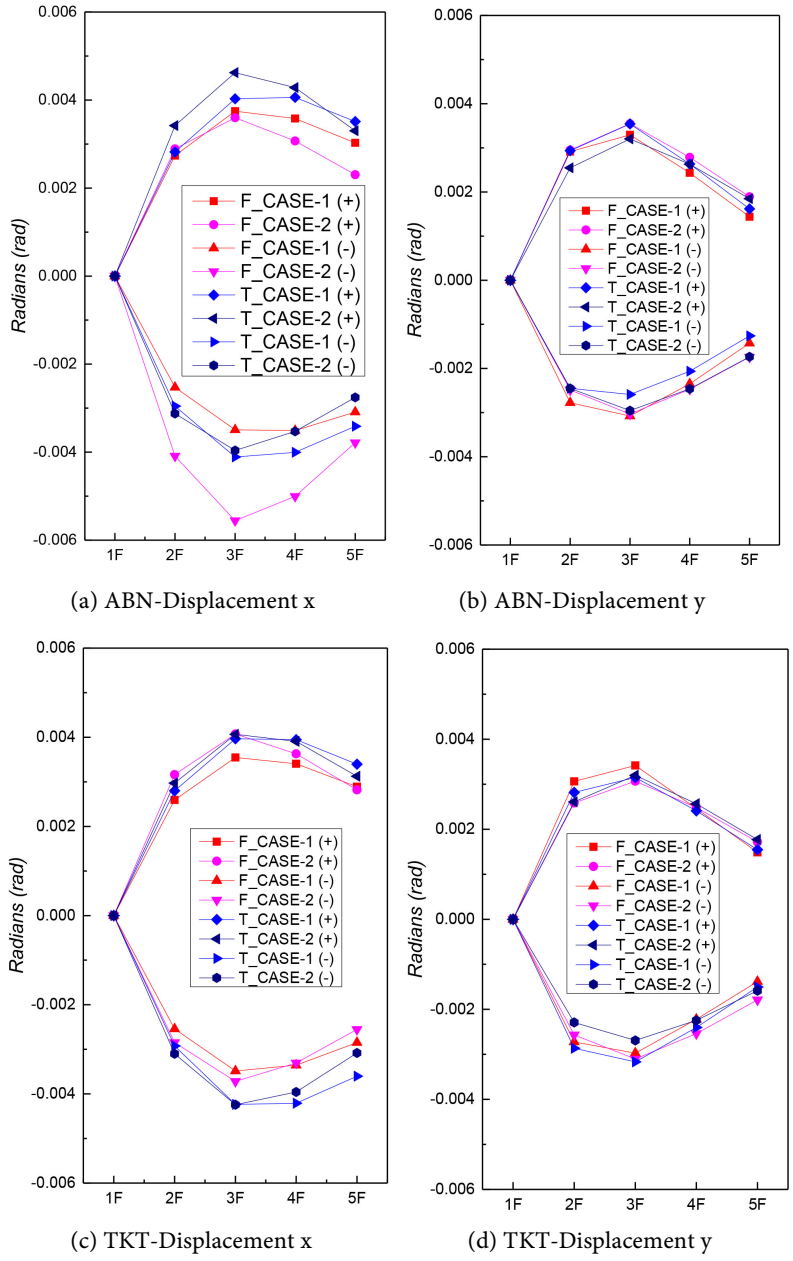

(a) ABN-Displacement x

(b) ABN-Displacement y

(c) TKT-Displacement x

(d) TKT-Displacement y

Figure 12. Average radians.

Further analysis, as illustrated in Figure 12, reveals that the radians vary significantly by story. Larger radians are observed in CASE-1 for the x-direction, indicating greater rotational movement, whereas CASE-2 exhibits larger radians in the y-direction. This pattern is consistently observed across the seismic waves from both Abeno and Takatori, highlighting the reliability of these findings.

These results underscore the importance of analyzing both displacement and radians to understand structural behavior under seismic conditions fully. The visual representations provided in Figure 11 and Figure 12 offer a clear and detailed comparison of how different column section designs respond to seismic forces, providing valuable insights for improving structural resilience in earth-

quake-prone areas.

3.3. Layer Displacement Angle

Figure 13 illustrates the results of average layer displacement angles for a specific RC frame structure, analyzed using nonlinear time history analysis based on two synthetic seismic waves from Abeno and Takatori. The graphs reveal both positive and negative average layer displacement angles.

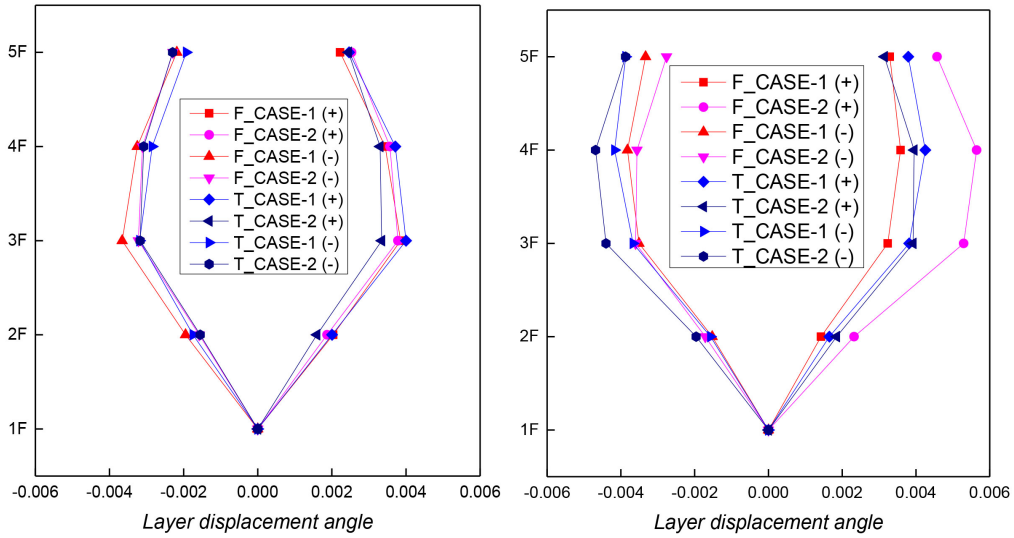

(a) ABN-Layer displacement angle-x

(b) ABN-Layer displacement angle-y

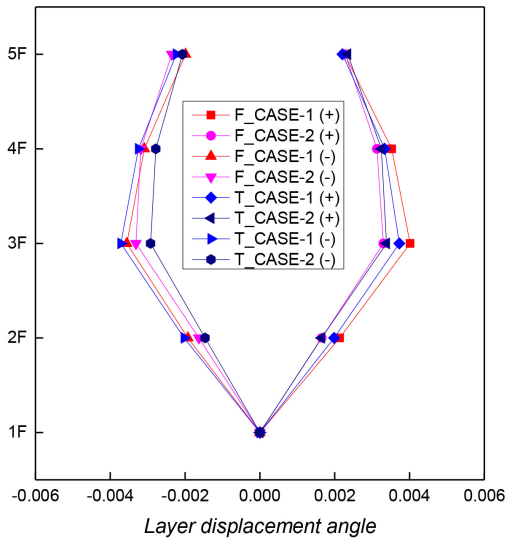

(c) TKT-Layer displacement angle-x

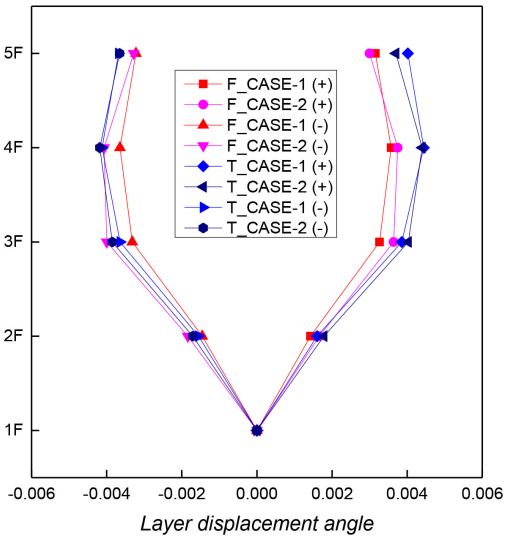

(d) TKT-Layer displacement angle-y

Figure 13. Layer displacement angle.

In the x direction, as shown in graphs (a) and (c), CASE-1 generally exhibits a larger average layer displacement angle compared to CASE-2. However, an intersection point occurred between the 3rd and 5th floors for both seismic waves from the Kobe 1995 earthquake in Abeno (ABN) and Takatori (TKT). This con-

sistent pattern across different seismic waves highlights a fundamental characteristic of the structural response. Conversely, in the y direction, depicted in graphs (b) and (d), CASE-2 demonstrates a larger average layer displacement angle than CASE-1. The intersection points in this direction are more pronounced, providing a clearer trend compared to the x-direction results. These intersections suggest that the different column section designs significantly impact the layer displacement angle.

Furthermore, the analysis indicates that the synthetic response spectrum based on the time domain reveals more distinct intersection points than the frequency domain counterpart. This observation implies that the temporal characteristics of seismic forces exert a more significant influence on the layer displacement angle than the frequency-based characteristics. This finding underscores the importance of considering both time and frequency domains in seismic analysis to understand the structural behavior under seismic loading.

3.4. Structural Displacement and Velocity

A crucial aspect of understanding the structural response under the seismic wave conditions of the Kobe 1995 earthquake is the comparison of the overall structural displacement with the original seismic waves from Abeno (ABN) and Takatori (TKT). This analysis aims to provide insights into how the structure behaves under these specific seismic conditions [9] [11]. **Figure 14** is pivotal in this analysis, as it visually presents the comparison of structural displacement for two different column section designs. By examining the displacements induced by the seismic waves from Abeno and Takatori, the figure helps illustrate the variations in structural response due to different seismic inputs and column section designs.

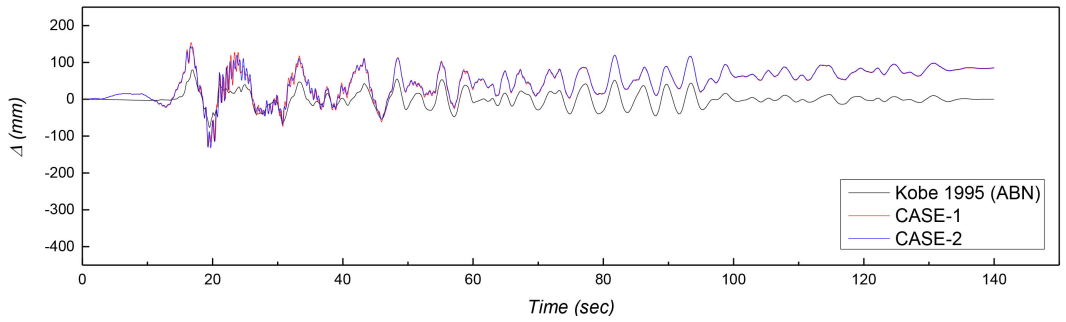

(a) Direction x—ABN

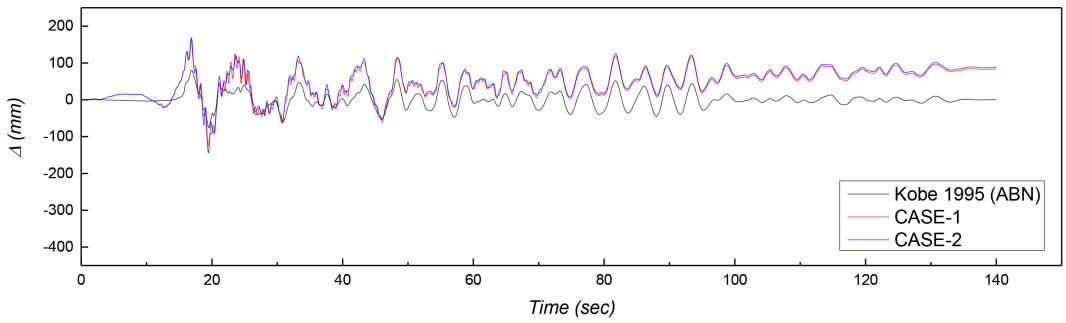

(b) Direction y—ABN

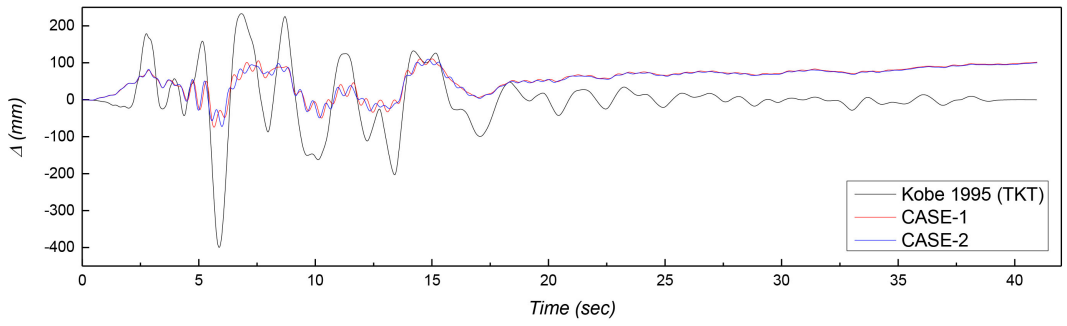

(c) Direction x—TKT

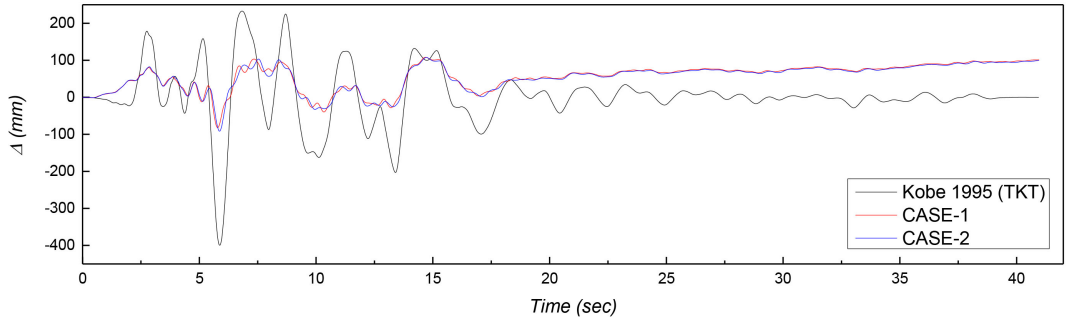

(d) Direction y—TKT

Figure 14. Structural seismic lateral displacement.

Graphs (a) and (c) in **Figure 14** specifically depict the structural displacement in the x-direction resulting from the seismic waves of Abeno and Takatori. This visual representation offers insights into the structural lateral movement and deformation that the structure experiences along the x-axis when subjected to the target seismic waves of the original seismic waves from the Kobe 1995 earthquake in Abeno (ABN) and Takatori (TKT). These graphs help to understand the extent of the lateral forces and their impact on the structural integrity during seismic events.

In parallel, graphs (b) and (d) in **Figure 14** illustrate the structural displacement in the y-direction. This depiction offers an examination of the structural lateral movement and deformation along the y-axis, providing a comprehensive understanding of how the structure responds to the seismic forces specified by both the original seismic waves of the Kobe 1995 earthquake in Abeno (ABN) and Takatori (TKT). These graphs highlight the extent of the structural response to lateral forces, helping to assess the impact of seismic events on the overall stability and integrity of the building.

As observed in graphs (a) and (c) in **Figure 14** along the x-direction, both specific cases under scrutiny reveal a pattern of irreversible structural displacement. This displacement becomes prominent from around 20 seconds in the seismic wave from Abeno (ABN) and from 6 seconds in the seismic wave from Takatori (TKT). This critical phase marks the occurrence of irreversible plastic damage to the target reinforced concrete (RC) frame structure in both CASE-1 and CASE-2 in the x-direction, highlighting the significant impact of these seis-

mic events on structural integrity and stability.

Examining the results along the y-direction as depicted in graphs (b) and (d) in Figure 14 reveals a phenomenon of irreversible structural displacement in both CASE-1 and CASE-2. The displacement in the y-direction also becomes prominent from around 20 seconds in the seismic wave from Abeno and from 6 seconds in the seismic wave from Takatori. This phenomenon signifies the occurrence of irreversible plastic damage to the target reinforced concrete (RC) frame structure in both CASE-1 and CASE-2. The consistent timing in the emergence of this irreversible displacement under each different seismic wave highlights the critical phase in understanding the structural behavior under seismic forces, underscoring the significant impact of these events on the overall structural integrity.

Analyzing Figure 14, which presents the structural lateral displacement graphs, reveals a noteworthy distinction between CASE-1 and CASE-2 over the duration of the specific seismic event. Although the graphical differences are not highly pronounced, a more detailed examination in Table 3 brings out a clear contrast. Specifically, for the reinforced concrete (RC) frame structure under consideration, CASE-1 exhibits longer structural displacement in the x-direction, while CASE-2 shows longer displacement in the y-direction. This phenomenon is consistent across both seismic waves from Abeno (ABN) and Takatori (TKT), underscoring the directional sensitivity of the structural response to the seismic forces.

Table 3. Result of structural displacement.

Types		CASE-1		CASE-2	
		Direction-x	Direction-y	Direction-x	Direction-y
		mm	mm	mm	mm
Abeno	Positive	153.81	165.76	143.80	168.72
	Negative	−132.25	−127.10	−131.73	−144.02
Takatori	Positive	110.57	107.60	109.92	108.04
	Negative	−74.34	−81.84	−72.45	−91.39

Graphs (a), (b), (c), and (d) in Figure 15 provide results of the structural velocity in the x and y directions, offering insights into the structure's response to the seismic wave of the Kobe 1995 earthquake from Abeno (ABN) and Takatori (TKT). Focusing on the x-direction, as presented in graphs (a) and (c), a notable observation is the occurrence of higher velocity values within the initial 15 to 30 seconds for the seismic wave from Abeno (ABN) and within the initial 5 to 7.5 seconds for the seismic wave from Takatori (TKT).

Analyzing the structural velocity in the y-direction, as presented in graphs (b) and (d) in Figure 15, highlights a noteworthy pattern of faster velocity within the initial 15 to 30 seconds for the seismic wave from Abeno (ABN) and within the initial 5 to 7.5 seconds for the seismic wave from Takatori (TKT). This temporal alignment of increased velocity is consistent with the observation of longer structural displacement in the y-direction during the same time period, as illus-

trated in Figure 14. This correlation provides deeper insights into the dynamic response of the structure under these specific seismic conditions, emphasizing the relationship between velocity and displacement during the critical initial phases of seismic activity.

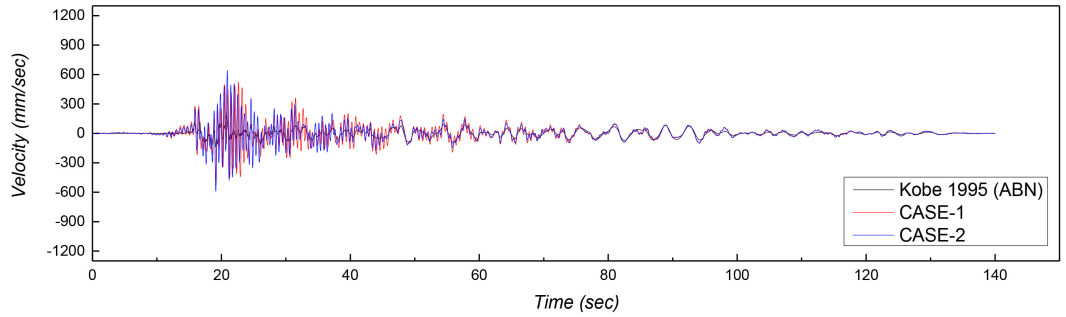

(a) Direction x—ABN

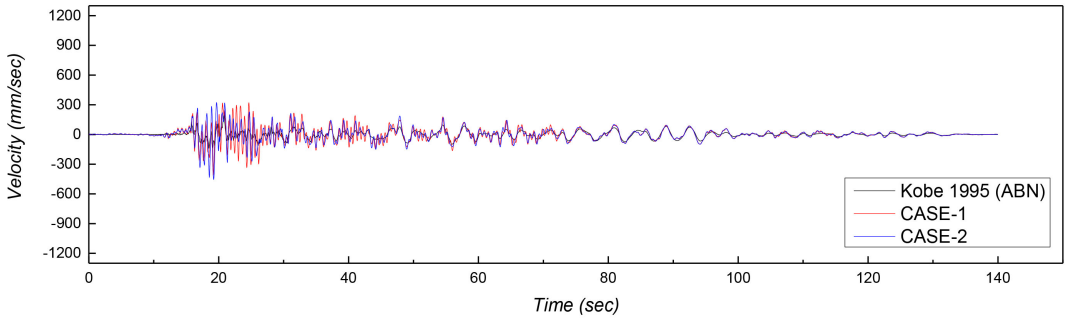

(b) Direction y—ABN

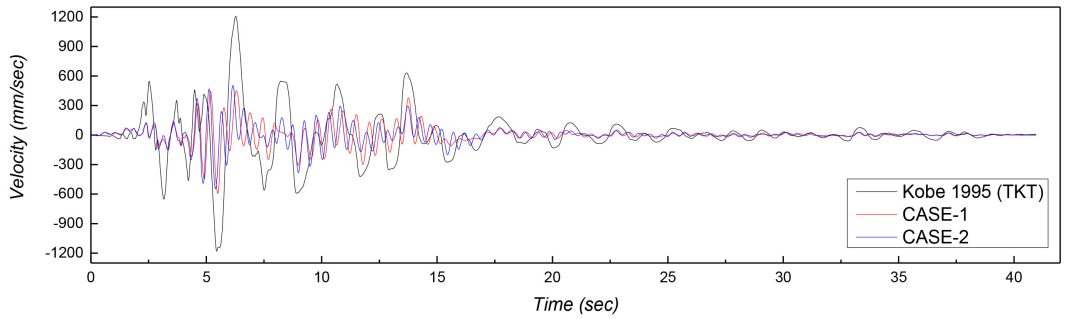

(c) Direction x—TKT

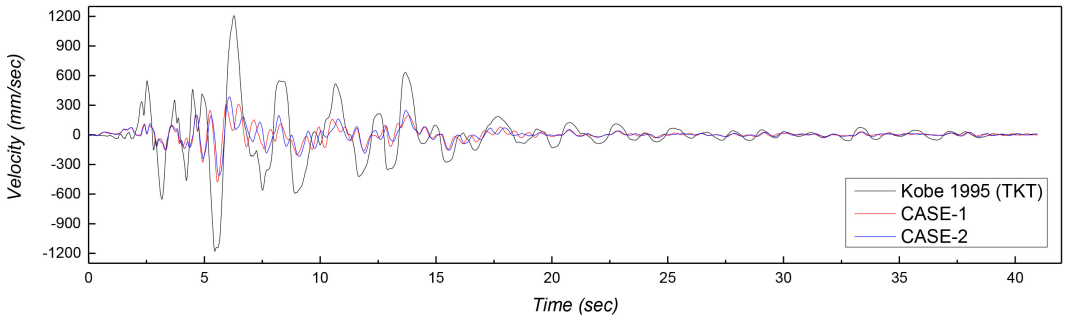

(d) Direction y—TKT

Figure 15. Structural seismic velocity.

The comparison of structural velocity between CASE-1 and CASE-2 in the context of the specific seismic event of Kobe 1995 is detailed in Table 4, reflecting the insights gained from the graphs in Figure 15. Specifically, for the reinforced concrete (RC) frame structure under consideration, CASE-1 exhibits faster structural velocity in the x-direction, while CASE-2 shows faster structural velocity in the y-direction. This pattern, similar to the results of structural lateral displacement, remains consistent across both seismic waves from Abeno (ABN) and Takatori (TKT), underscoring the directional sensitivity of the structural response to seismic forces. Also, this consistent directional behavior highlights the impact of column section design on the structural performance during seismic events.

Table 4. Result of structural velocity.

Types		CASE-1		CASE-2	
		Direction-x	Direction-y	Direction-x	Direction-y
		mm/sec	mm/sec	mm/sec	mm/sec
Abeno	Positive	641.42	320.31	522.57	322.42
	Negative	−590.78	−411.95	−515.61	−454.66
Takatori	Positive	450.88	312.53	503.74	384.27
	Negative	−592.26	−477.12	−546.59	−410.23

4. Summary of the Analysis

This research focuses on the seismic analysis of a typical educational RC frame structure at Kyungpook National University, employing two different seismic waves from Abeno (ABN) and Takatori (TKT). The primary goal is to evaluate the structural performance under these seismic conditions, specifically examining the impact of different column orientations. By concentrating on varying column orientations, the study aims to provide a detailed understanding of how column configurations influence seismic performance [10]. By comparing the structural responses to the two distinct seismic waves, the findings are expected to highlight the effects of these seismic waves and elucidate the application of synthetic seismic methods in nonlinear time history analysis [1] [9] [11].

The findings from the nonlinear time history analysis underscore that longer column sections aligned with the load direction consistently exhibit superior performance across several parameters. Specifically, these sections demonstrate larger base shear force and base moment, while simultaneously experiencing shorter displacements. This indicates that longer column sections are more effective in handling seismic loads, as they generate higher base shear and moments but result in reduced displacement, thereby enhancing the overall structural stability during seismic events.

Moreover, the analysis extends to discussing average layer displacement angles, average displacement, and radians. The findings consistently show that

longer column sections aligned with the load direction exhibit superior characteristics, such as smaller layer displacement angles and shorter displacements. This suggests that these section designs are better able to withstand larger radians under seismic conditions. Furthermore, the discussion highlights an intersection from the 3rd to the 5th floor in the analysis of radians and average layer displacement angle, emphasizing the substantial influence of the number of stories on the radians of the joints in the RC frame structure. This intersection underscores how the structural response varies with height, particularly affecting joint behavior and overall stability during seismic events.

The comparison between two approaches for synthesizing response spectrum—frequency domain and time domain—based on nonlinear time history analysis reveals a strong correlation in the results for base shear and base moment using the time domain. This indicates that the synthetic response spectrum with the time domain provides a more accurate structural analysis compared to the frequency domain method. This observed phenomenon is consistent across various results, including average displacement, radians, and average layer displacement angle. The findings suggest that employing the time domain in synthetic response spectrum analysis significantly enhances the precision of structural evaluation.

The results of structural lateral displacement and velocity underscore the significance of longer column sections oriented with the load direction, revealing a notable reduction in structural lateral displacement and slower structural velocity. This implies that longer column sections demonstrate heightened resilience against extensive lateral displacement and rapid structural velocity, especially under seismic conditions. Such findings illuminate the pivotal role of column design in mitigating structural vulnerability and enhancing seismic resilience. By aligning with the load direction, longer column sections effectively distribute and absorb seismic forces, thereby minimizing lateral displacement and velocity, which are crucial factors in ensuring structural stability and safety during seismic events.

The comparative analysis of the structural responses to the seismic waves from Abeno (ABN) and Takatori (TKT) reveals that, despite Takatori's generally higher seismic intensity, there are minimal differences in the results. This consistency is observed under both the frequency and time domain synthetic approaches in nonlinear time history analysis. The findings primarily reflect the target response spectrum of KBC 2016, rather than the variations in seismic intensity between the two seismic waves. This outcome highlights the critical importance of the target response spectrum in the nonlinear time history analysis. The emphasis on the target response spectrum suggests that it plays a more pivotal role than the reference acceleration time history in accurately predicting structural performance and ensuring robust seismic design based on the seismic wave synthetic method in nonlinear time history analysis.

Moreover, when comparing the seismic responses of Abeno (ABN) and Takatori (TKT), it is evident that Abeno's seismic wave, despite having a smaller

seismic intensity, results in a slightly larger base shear force, longer displacement, and greater average displacement angle. This observation underscores the impact of a longer seismic wave period on structural fatigue. The longer duration of the seismic waves from Abeno (ABN) appears to contribute to increased structural fatigue, which in turn leads to more significant structural damage. This finding highlights the critical role that the period of a seismic wave plays in influencing structural performance, suggesting that even lower-intensity waves can cause considerable damage if their duration is extended.

5. Conclusions

In this research, the discussion covers various aspects such as base shear, base moment, layer displacement, layer radians, layer displacement angle, and structural lateral displacement. It emphasizes that aligning the column section orientation with the load direction in an RC frame structure can significantly enhance structural performance during seismic events.

Moreover, regarding the nonlinear time history analysis under the seismic waves synthetic approach, this research explains that the choice of the target response spectrum is more significant than considering the variations in seismic intensity between different seismic waves. Therefore, compared to the selection of seismic waves, selecting the appropriate target response spectrum is more meaningful for the approach of synthetic seismic waves within nonlinear time history analysis.

Throughout the nonlinear time history analysis using the seismic waves synthetic approach, it is evident that this method is a crucial component of Nonlinear Dynamic Analysis (NDA). The findings, particularly regarding structural lateral displacement, underscore the significance of nonlinear time history analysis. This method effectively reveals the dynamic behavior of structures under seismic events, providing valuable insights into their performance and resilience.

The findings of this research are anticipated to be a significant resource for structural design, specifically focusing on the impact of different column section orientations. Additionally, these insights are expected to guide seismic reinforcement efforts for existing RC buildings. By providing detailed analysis and data, this research aims to enhance the understanding of structural performance under seismic conditions, ultimately contributing to more resilient and durable building designs.

Acknowledgements

The research described in this paper was financially supported by Shanghai HaXell elevator and performed at Kyungpook National University.

Conflicts of Interest

The authors declare no conflicts of interest regarding the publication of this paper.

References

[1] Hosseini, M., Hashemi, B. and Safi, Z. (2017) Seismic Design Evaluation of Reinforced Concrete Buildings for Near-Source Earthquakes by Using Nonlinear Time History Analyses. *Procedia Engineering*, **199**, 176-181. https://doi.org/10.1016/j.proeng.2017.09.225

[2] Çavdar, Ö. and Bayraktar, A. (2013) Pushover and Nonlinear Time History Analysis Evaluation of a RC Building Collapsed during the Van (Turkey) Earthquake on October 23, 2011. *Natural Hazards*, **70**, 657-673. https://doi.org/10.1007/s11069-013-0835-3

[3] Kojiro, I., Tomotaka, I., Haruko, S., Arben, P. and Katsuhiro, K. (1997) Lesson from the 1995 Hyogo-Ken Nanbu Earthquake: Why Were Such Destructive Motions Generated to Buildings. *Journal of Natural Disaster Science*, **17**, 99-127.

[4] Wald, D.J. (1996) Slip History of the 1995 Kobe, Japan, Earthquake Determined from Strong Motion, Teleseismic, and Geodetic Data. *Journal of Physics of the Earth*, **44**, 489-503. https://doi.org/10.4294/jpe1952.44.489

[5] Motosaka, M. and Nagano, M. (1996) Analysis of Ground-Motion Amplification Characteristics in Kobe City Considering a Deep Irregular Underground Structure. Interpretation of Heavily Damaged Belt Zone during the 1995 Hyogo-Ken Nanbu Earthquake. *Journal of Physics of the Earth*, **44**, 577-590. https://doi.org/10.4294/jpe1952.44.577

[6] Takai, N., Shigefuji, M., Horita, J., Nomoto, S., Maeda, T., Ichiyanagi, M., *et al.* (2019) Cause of Destructive Strong Ground Motion within 1-2 S in Mukawa Town during the 2018 Mw 6.6 Hokkaido Eastern Iburi Earthquake. *Earth, Planets and Space*, **71**, Article No. 67. https://doi.org/10.1186/s40623-019-1044-4

[7] Mylonakis, G., Syngros, C., Gazetas, G. and Tazoh, T. (2006) The Role of Soil in the Collapse of 18 Piers of Hanshin Expressway in the Kobe Earthquake. *Earthquake Engineering & Structural Dynamics*, **35**, 547-575. https://doi.org/10.1002/eqe.543

[8] Betti, M., Galano, L. and Vignoli, A. (2015) Time-History Seismic Analysis of Masonry Buildings: A Comparison between Two Non-Linear Modelling Approaches. *Buildings*, **5**, 597-621. https://doi.org/10.3390/buildings5020597

[9] Nguyen, P. and Kim, S. (2014) Nonlinear Inelastic Time-History Analysis of Three-Dimensional Semi-Rigid Steel Frames. *Journal of Constructional Steel Research*, **101**, 192-206. https://doi.org/10.1016/j.jcsr.2014.05.009

[10] Mahapara, F. and Sakshi, G. (2017) A Critical Evaluation of the Effect of Soft Storey and Column Orientation on RC Buildings. *International Journal of Science Technology & Engineering*, **3**, 44-47.

[11] Yusra, A., Mustafa, A., Refiyanni, M. and Zakia, Z. (2023) Performance Structural Analysis of U2C Building with the Kobe Earthquake Spectrum. *International Journal of Engineering, Science and Information Technology*, **3**, 36-46. https://doi.org/10.52088/ijesty.v3i1.413

[12] Hakim, R.A., Alama, M.S.A. and Ashour, S.A. (2014) Seismic Assessment of an RC Building Using Pushover Analysis. *Engineering, Technology & Applied Science Research*, **4**, 631-635. https://doi.org/10.48084/etasr.428

[13] Pednekar, S.C., Chore, H.S. and Patil, S.B. (2015) Pushover Analysis of Reinforced Concrete Structures. *International Conference on Advancements in Engineering and Technology*, *IISRT*, Chennai, 17 November 2015, 7-10.

[14] Wei, B., Yan, L., Jiang, L., Hu, Z. and Li, S. (2021) Errors of Structural Seismic Responses Caused by Frequency Filtering Based on Seismic Wave Synthesis. *Soil Dy-*

namics and Earthquake Engineering, **149**, Article ID: 106862.
https://doi.org/10.1016/j.soildyn.2021.106862

[15] Schuberth, B.S.A., Zaroli, C. and Nolet, G. (2012) Synthetic Seismograms for a Synthetic Earth: Long-Period P- and S-Wave Traveltime Variations Can Be Explained by Temperature Alone. *Geophysical Journal International*, **188**, 1393-1412.
https://doi.org/10.1111/j.1365-246x.2011.05333.x